Understanding the potential of climate teleconnections to project future groundwater drought

Rust, William.[a]; Holman, Ian.[a]; Bloomfield, John.[b]; Cuthbert, Mark.[c]; Corstanje, Ron.[d]

a Cranfield Water Science Institute (CWSI), Cranfield University, Bedford MK43 0AL
b British Geological Survey, Wallingford, OX10 8ED
c School of Earth and Ocean Sciences, Cardiff University, Park Place, Cardiff, CF10 3AT
d Centre for Environment and Agricultural Informatics, Cranfield University, Bedford MK43 0AL

Abstract

Predicting the next major drought is of paramount interest to water managers, globally. Estimating the onset of groundwater drought is of particular importance, as groundwater resources are often assumed to be more resilient when surface water resources begin to fail. A potential source of long-term forecasting is offered by possible periodic controls on groundwater level via teleconnections with oscillatory ocean-atmosphere systems. However, relationships between large-scale climate systems and regional to local-scale rainfall, ET and groundwater are often complex and non-linear so that the influence of long-term climate cycles on groundwater drought remains poorly understood. Furthermore it is currently unknown whether the absolute contribution of multi-annual climate variability to total groundwater storage is significant. This study assesses the extent to which multi-annual variability in groundwater can be used to indicate the timing of groundwater droughts in the UK. Continuous wavelet transforms show how repeating teleconnection-driven 7-year and 16-32 year cycles in the majority of groundwater sites from all the UK's major aquifers can systematically control the recurrence of groundwater drought; and we provide evidence that these periodic modes are driven by teleconnections. Wavelet reconstructions demonstrate that multi-annual periodicities of the North Atlantic Oscillation, known to drive North Atlantic meteorology, comprise up to 40% of the total groundwater storage variability. Furthermore, the majority of UK recorded droughts in recent history coincide with a minima phase in the 7-year NAO-driven cycles in groundwater level, providing insight into drought occurrences on a multi-annual timescale. Long-range groundwater drought forecasts via climate teleconnections present

transformational opportunities to drought prediction and its management across the North Atlantic region.

1. Introduction

Multi-annual variability detected in hydrometeorological datasets has long been associated with systems of atmospheric-oceanic (climatic) oscillation, such as El Niño Southern Oscillation (ENSO) and the North Atlantic Oscillation (NAO). Such periodic teleconnection signals have been detected in rainfall (Luković et al. 2014), evapotranspiration (Tabari et al. 2014), air temperature (Faust et al. 2016), and river flow (Su et al. 2018; Dixon, et al. 2011); however these periodicities are often weak when compared to the finer-scaled (daily to seasonal) variability that is typical of hydrometeorological processes (Meinke et al. 2005). By contrast, groundwater systems are expected to be particularly susceptible to multi-annual teleconnection influence, given their sensitivity to long-term changes in rainfall and evapotranspiration (Bloomfield & Marchant 2013a; Forootan et al. 2018; Van Loon 2015; Folland et al. 2015), and their ability to filter fine-scale variability in recharge signals (Dickinson et al. 2014; Velasco et al. 2015; Townley 1995). Consequently, recent studies have focused on the detection of long-term periodic cycles in groundwater levels in Europe (e.g. Holman et al. 2009; Holman et al. (2011); Folland et al. (2015); and Neves et al. (2019)), North America (e.g. Tremblay et al. (2011); Kuss & Gurdak (2014)) and globally (e.g. Wang et al. (2015); Lee & Zhang (2011)), and their relationships with climatic oscillations. An understanding of multi-annual perioidicity strength in groundwater level may provide an improvement in long-lead forecasting of hydrogeological extremes (Rust et al. 2018; Meinke et al. 2005; Kingston et al. 2006), in part, by enabling such cyclical behaviour to be projected into the future. This is particularly apparent of groundwater drought, which is known to result from multi-annual moisture deficits (Van Loon 2015; Van Loon et al. 2014; Peters et al. 2006). Therefore, it is critical to quantify the absolute strength of all periodicities within groundwater levels so that

the strength of multi-annual cycles, the influence of teleconnections, and their contribution towards groundwater droughts can be understood.

Existing studies into groundwater teleconnections use quantitative methods to detect periodic behaviour in groundwater datasets and often their relationship with time series of climate indices (used to measure the strength and state of climate oscillations). Common quantitative methods range from temporal correlation analysis (Knippertz et al. 2003; Szolgayova et al. 2014) to more complex periodicity detection and comparison. These latter methods include Fourier transform, (Nakken, 1999, Pasquini et al. 2006), singular spectrum analysis (SSA) (Kuss & Gurdak 2014; Neves et al. 2019) and wavelet transformations (Fritier et al. 2012; Holman et al. 2011; Tremblay et al. 2011). The wavelet transform (WT) has been shown to be particularly skilful at detecting multi-annual periodic behaviour in noisy hydrogeological datasets; detecting the influence of the NAO, ENSO and Atlantic Multidecadal Oscillation (AMO) on North American groundwater levels (Kuss & Gurdak 2014; Velasco et al. 2015), and the NAO, East Atlantic pattern (EA) and Scandinavian pattern on European groundwater level variability (Holman et al. 2011; Neves et al. 2019). However, in order to enhance multi-annual periodicity detection, many studies have used data processing methods that remove or supress variability at the higher end of the frequency spectrum (e.g. winter or annual averaging or conversion of time series to cumulative departures from mean (Weber & Stewart 2004)). Due to this data modification, it is currently unknown whether the absolute contribution of multi-annual climate variability to total groundwater storage is significant. This limitation makes assessment of systematic linkages between climatic oscillations and groundwater level response problematic (Rust et al. 2018). As a result, the fundamental question of whether multi-annual teleconnection cycles in groundwater level are sufficiently strong to influence hydrogeological drought remains largely unanswered. Given the potential for improved long-lead forecasting, quantification of multi-annual variability in groundwater level represents an opportunity to support efficient infrastructure investment, systems of water trading (Rey et al. 2018) and robust planning for groundwater drought.

The aim of this paper is to assess the extent to which periodic behaviour in groundwater level produced by teleconnections, may be used as an indicator for the timing of groundwater droughts. In doing so, this paper develops and applies an improved method to describe and characterise the absolute strength of periodic behaviour in groundwater level and its drivers (rainfall and evapotranspiration). This aim will be met by addressing the following research objectives:

1. Characterise dominant intra- and multi-annual periodicities in groundwater level records across a range of aquifer types
2. Quantify the absolute strength of these multi-annual periodic groundwater level oscillations compared to the total variability in groundwater levels
3. Qualitatively assess evidence for the control of climate teleconnections on identified multi-annual periods
4. Assess the extent to which the timing of the multi-annual periodic groundwater level oscillations align with recorded groundwater droughts

These objectives will be implemented on UK hydrogeology records, given the considerable coverage of recorded groundwater level data in time and across the country (Marsh & Hannaford 2008) however the methodologies developed can be applied to any regions.

5. Data and Methods

2.1. Groundwater data

Groundwater level time series from 59 reference boreholes covering all of the major UK aquifers, with record lengths of more than 20 years and data gaps no longer than 24 months, have been assessed in the study. These recorded groundwater level hydrographs range from 21 to 181 years in length, with an average length of 53 years. The sites are part of the British Geological Survey's Index Borehole network and, in addition to their data coverage, have been chosen as they exhibit representative and naturalistic hydrographs with minimal impact from

abstractions. They cover a range of unconfined and confined consolidated aquifer types and have been categorised into 5 main aquifer groups; 34 records in Chalk, a limestone aquifer comprising of a dual porosity system with localized areas where it exhibits confined characteristics; 8 records in Limestone, characterised by fast-responding fracture porosity; 3 records in Oolite characterised by highly fractured lithography with low intergranular permeability; 12 sites in Sandstone, comprised of sands silts and muds with principle inter-granular flow but fracture flow where fractures persist; and 2 records in Greensands, characterised by intergranular flow with lateral fracture flow depending on depth and formation (Marsh & Hannaford 2008).

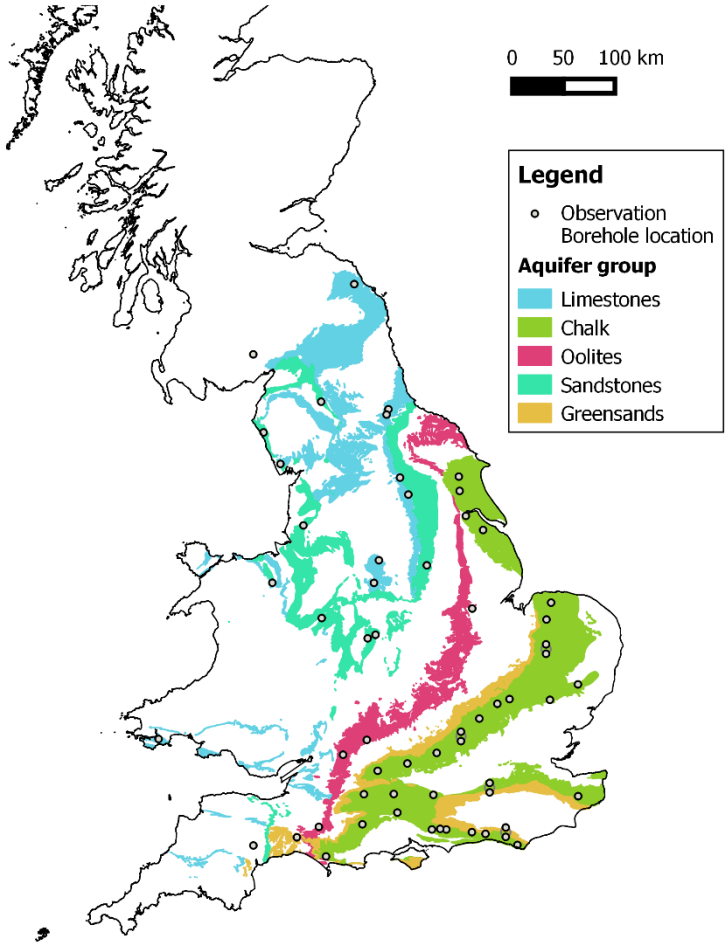

120

121 *Figure 1 - Location of the observation borehole locations used in this study. Boreholes within 0.5 km of another*
122 *have been displaced and denoted on a grey circle for visibility.*

123

124 ## 2.2. Rainfall

125 Rainfall time series from the Centre of Ecology and Hydrology's CEH-GEAR 1km gridded
126 rainfall dataset (Tanguy et al. 2016), which is based on spatio-temporal interpolation of daily
127 rain gauge totals between 1890 and 2017, was used. However, relatively few rainfall stations
128 exist prior to 1950 that were used for this interpolation; as such data prior to 1950 was not
129 used in this analysis. Monthly rainfall series have been calculated for each borehole from the
130 1km grid cell in which they are located, as geospatial data on areas of groundwater recharge
131 connected to specific observation boreholes does not exist. This dataset may contain artefacts
132 as a result of the spatio-temporal interpolation, in comparison to station data. However the
133 use of rainfall data in this study is to provide a broad understanding of rainfall periodicities to

supplement those from groundwater level data. As such, this interpolated dataset is deemed appropriate.

2.3. Potential Evapotranspiration (PET)

Monthly PET series for each borehole have been derived from the Centre of Ecology and Hydrology's CHESS-PE 1km gridded dataset of calculated daily PET values. The PET values, between 1960 and 2015, were calculated using the Penman-Monteith equation, with meteorological data taken from the CHESS gridded meteorological dataset. Details on the underlying observation datasets and interpolation methods can be found in Robinson et al. (2016). This data has been used previously to study long-term trends in hydrological variability (Robinson et al. 2017).

2.4. Methods

2.4.1. Data pre-processing

In this study we use the continuous wavelet transform (CWT) to produce a time-averaged frequency spectrum for each borehole hydrograph and co-located rainfall and PET time series.

For all datasets, gaps less than two years were infilled using a cubic spline to produce a complete time series for the CWT. This interpolated information was later removed from the time-frequency transformation (prior to time-averaging) to ensure that the data infilling had minimal effect on the final spectrum. For time series with gaps greater than two years, the shortest time period before or after the data gap was removed to produce one complete record. Individual rainfall and PET time series were trimmed to match the length of the corresponding borehole level time series. All time series were centred on the long-term mean and normalized to the standard deviation to produce a time series of anomalies. Unlike most previous studies, no high- or low-band filtering was undertaken on the datasets, ensuring all

159 information on periodic variability was preserved. This approach ensures that the Proportion
160 of a periodicity to the variance (standard deviation) of the original dataset is not modified.

161 2.4.2. Continuous Wavelet Transform.

162 Following the data pre-processing steps, a CWT was applied to quantify the time-averaged
163 frequency spectra of the rainfall, PET and groundwater datasets. The CWT has been used
164 to assess long term trends and periodicities in many hydrological datasets including rainfall
165 (Rashid et al. 2015), river flow (Su et al. 2017), and groundwater (Holman et al. 2011; Kuss
166 & Gurdak 2014). We use the package "WaveletComp" produced by Rosch & Schmidbauer
167 (2018) for all transformations in this paper.

168 The continuous wavelet transform, W, consists of the convolution of the data sequence (x_t)
169 with scaled and shifted versions of a mother wavelet (daughter wavelets):

$$W(\tau, s) = \sum_t x_t \frac{1}{\sqrt{s}} \psi * \left(\frac{t - \tau}{s}\right) \quad \text{(Eq. 1)}$$

170 where the asterisk represents the complex conjugate, τ is the localized time index, s is the
171 daughter wavelet scale and dt is increment of time shifting of the daughter wavelet. The
172 choice of the set of scales s determines the wavelet coverage of the series in its frequency
173 domain. The Morlet wavelet was favoured over other candidates due to its good definition in
174 the frequency domain and its similarity with the signal pattern of the environmental time
175 series used (Tremblay et al. 2011; Holman et al. 2011).

176 The CWT produces a time-frequency wavelet power spectrum for each time series. Within
177 the time-frequency spectra, a cone of influence (COI) is used to denote those parts that are
178 affected by edge-effects, where estimations of spectral power are less accurate. Therefore
179 only data from within COI were averaged over time to produce a time-average wavelet power
180 spectrum for frequency bands from 6 months up to 64 years. Wavelet power spectra were
181 then normalised to the maximum average wavelet value so that the frequency distribution of
182 each site can be directly compared. The normalized average wavelet power spectra (herein

183 referred to as the wavelet power spectra) provide a comparative measure of the strength of
184 the range of periodicities within frequency space.

185 2.4.3. Significance testing

186 As Allen and Smith (1996) demonstrate, geophysical datasets can exhibit pseudo-periodic
187 behaviour as a result of their lag-1 autocorrelation (AR1) properties. Datasets with greater
188 AR1 tend to have spectra biased towards low frequencies, thus they are described as
189 containing red noise (Allen et al. 1996; Meinke et al. 2005; Velasco et al. 2015). In order to
190 assess the likelihood that a periodic signal is the result of internal (red) noise within the data,
191 significance of the red noise null hypothesis was tested. For this, 1000 randomly constructed
192 synthetic series with the same AR1 as the original time series were created using Monte Carlo
193 methods. Wavelet spectra maxima from these represent periodicity strength that can arise
194 from a purely red noise process. Wavelet powers from the original dataset that are greater
195 than these “red” periodicities are therefore considered to be driven by a process other than
196 red noise, thus rejecting the null hypothesis. Here, while a 95% Confidence Interval (CI) (<=
197 0.05 alpha values) is identified, we report on the full range of alpha results to provide a detailed
198 assessment of the likelihood of external forcing on periodic behaviour.

199 2.4.4. Time reconstruction

200 In order to assess the characteristics of periodicities over time, we employ a reversal of the
201 wavelet transform (wavelet reconstruction) to convert selected periodic domains back into a
202 time series of normalised anomalies. Period bands were selected where the frequency spectra
203 identified shared wavelet power (and significance) between groundwater, rainfall and PET,
204 indicating a wide-spread signal presence at these bands.

205 The reverse wavelet transform is given by:

$$(x_t) = \frac{dj \cdot dt^{1/2}}{0.776 \cdot \psi(0)} \sum_s \frac{Re(W(.,s))}{s^{1/2}} \quad \text{(Eq. 2)}$$

206 Where *dj* is the frequency step and *dt* is the time step.

Negative phases of these time-reconstruction anomaly time series were compared to episodes of recorded wide-scale hydrogeological drought (provided by Marsh et al. (2007) and Todd et al. 2013)), to assess the relationships between multi-annual variability in groundwater and groundwater droughts.

2.3.5 Periodicity strength quantification

While the wavelet power spectra from the CWT provide an estimate of the relative strength of periodicities compared to the total frequency spectra, they do not provide an absolute measure of a periodicities contribution to total groundwater variability (which includes noise and non-periodic information). As such the percentage contributions of each time-reconstruction have been calculated. Since the datasets were normalised to the standard deviation of the raw data prior to the CWT, the standard deviations of the reconstructed anomaly time series represent the proportion of the original standard deviation as a decimal percentage.

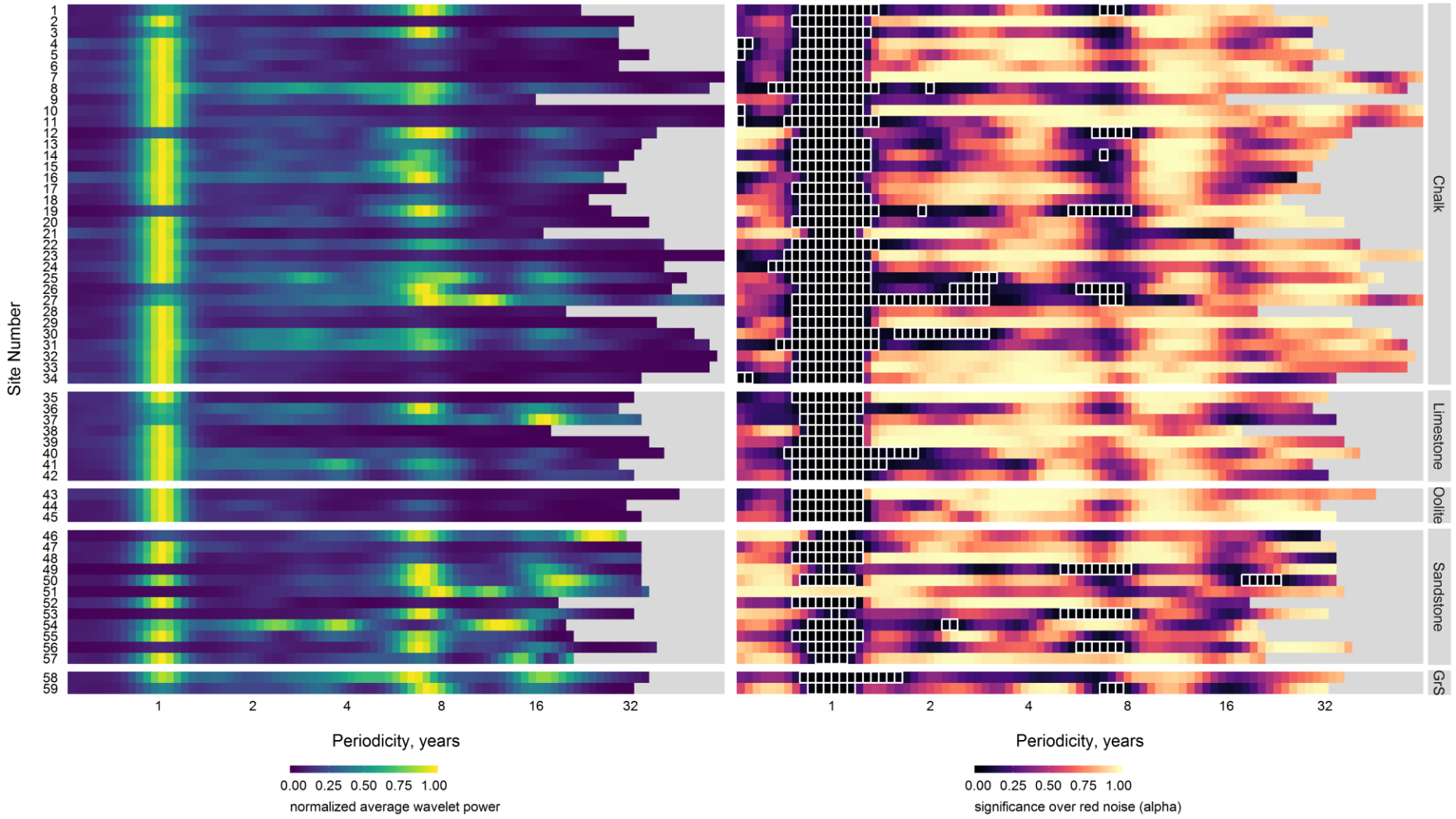

Figure 2 - Normalised average wavelet power spectra (left) and wavelet power significance alphas (right) for monthly groundwater levels in the 59 index boreholes (grouped by aquifer type). In the right-hand figure, boxes outlined in white are those powers that are significant over red noise to a 95% confidence interval (a <= 0.05).

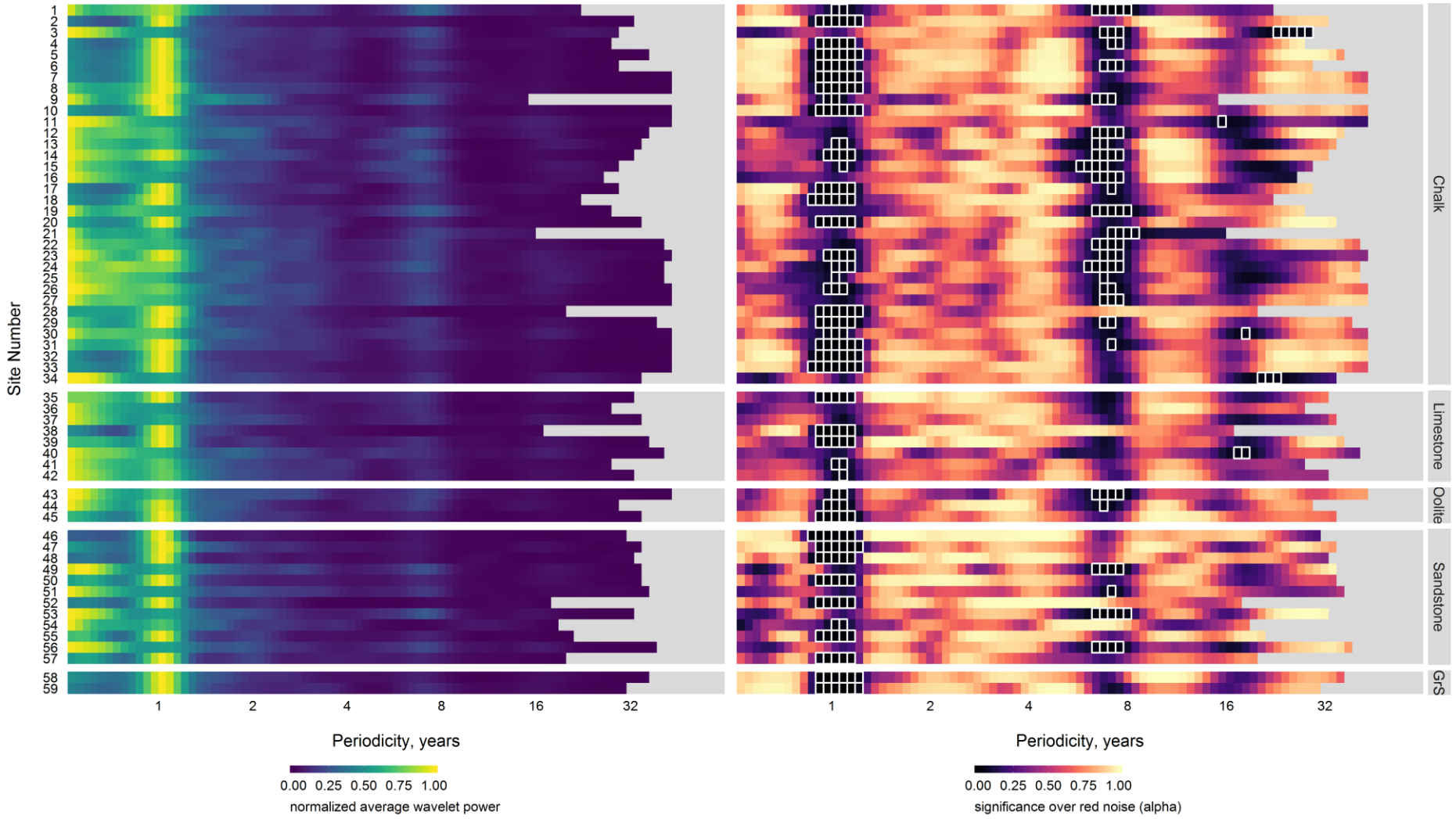

Figure 3 - Normalised average wavelet power spectra (left) and wavelet power significance alphas (right) for monthly rainfall time series for co-locations of the 59 index boreholes. In the right-hand figure, boxes outlined in white are those powers that are significant over red noise to a 95% confidence interval (a <= 0.05).

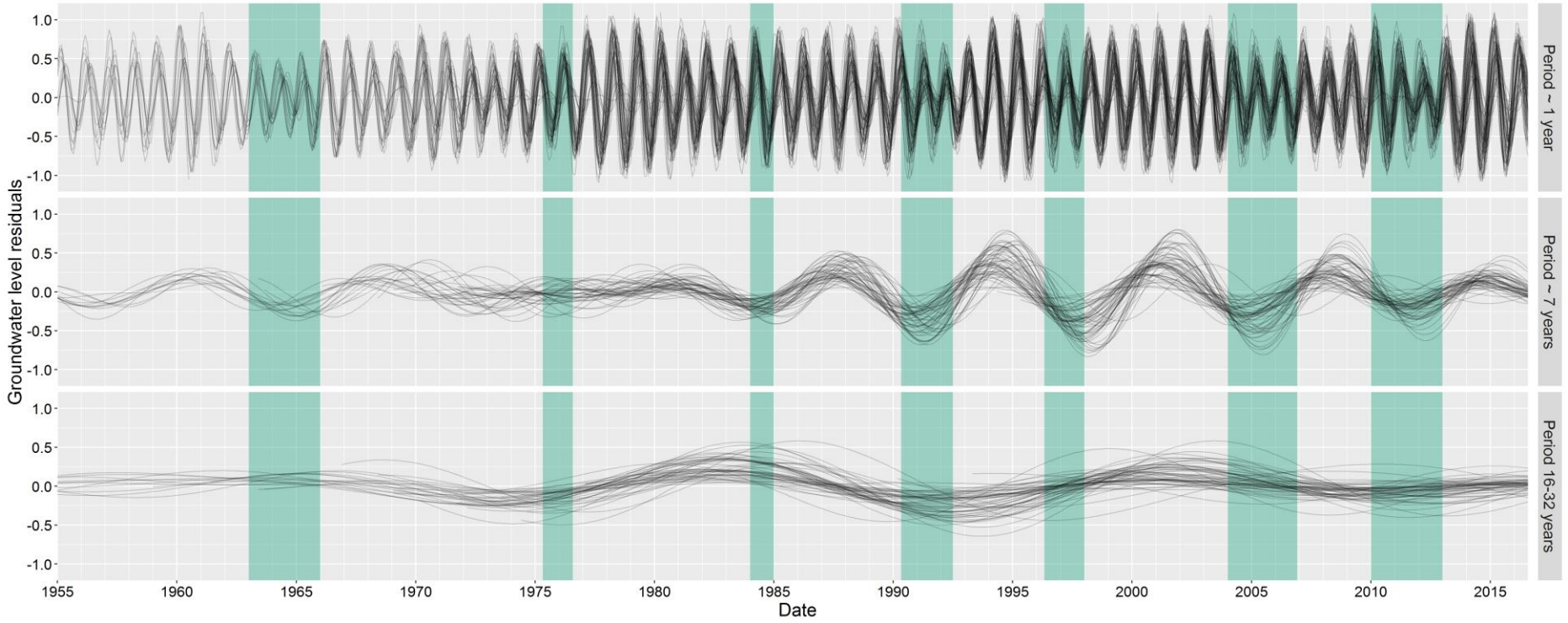

Figure 4 – Overlaid reconstructions of the three key periodic domains found across the 59 groundwater wavelet spectra are shown. All periods (both significant and non-significant) within these bands have been displayed to allow for comparison of period strength and phase over time. Areas shaded blue represent approximate periods of significant droughts in the UK. Only reconstructions between 1955 and 2017 are shown to allow clearer comparison.

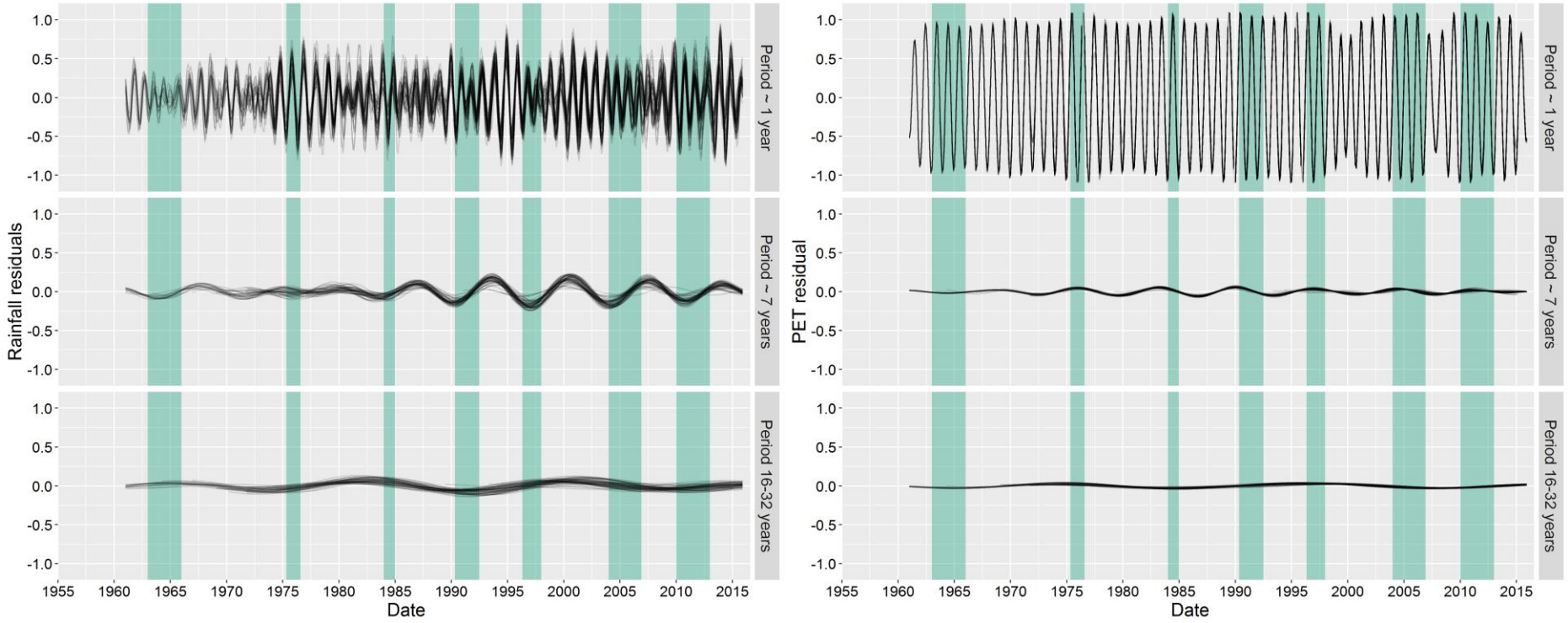

Figure 5 – Overlaid rainfall (left) and PET (right) reconstructions of the three key periodic domains are shown. All periods (both significant and non-significant) within these bands have been displayed to allow for comparison of period strength and phase over time. Areas shaded blue represent approximate periods of significant droughts in the UK. Only reconstructions between 1955 and 2017 are shown to allow clearer comparison.

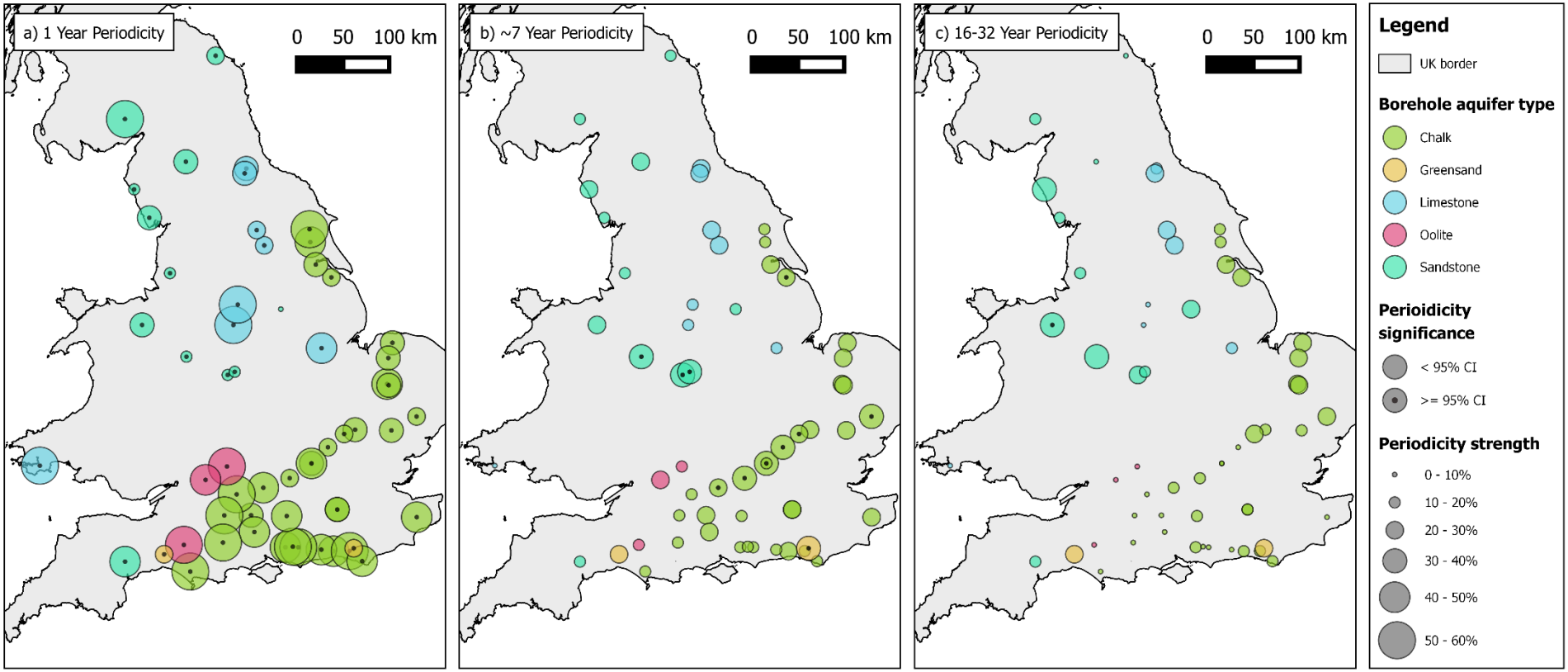

236

237 *Figure 6 – Maps showing strength (percentage of the original time series standard deviation) and significance of the a) 1 year, b) ~7 year and c) 16-32 year periodicity bands.*

238 *No periodicity strength was found to be above 60% of the original signal.*

3. Results

3.1. Time-averaged wavelet power and significance over red noise

Wavelet power spectra (frequency strength) and alpha values (significance) for each of the 59 groundwater level and rainfall time series are displayed in figures 2 and 3 respectively. Wavelet power is analogous to the strength of the periodicity compared to other frequencies. Periodicities with alpha values less than or equal to 0.05 (95% CI) are highlighted. Bands of greater wavelet power and lower alpha values at periodicities of 1, ~7 and 16-32 year(s) can be seen across the majority of the groundwater and rainfall spectra for the 59 sites (herein referred to as P1, P7 and P16-32 respectively). PET wavelet spectra were found to have no notable or significant periodicity beyond seasonality (indicative of the UK's temperate climate), and are displayed in the supplementary material.

The annual cycle (P1) exhibited the greatest power across 43 of the 59 observation borehole spectra, with normalised wavelet powers ranging from 0.03 to 1 (mean of 0.84). Alpha values for P1 in the observation boreholes also showed the greatest likelihood of external forcing when compared to the other identified periodic domains (alpha values ranging from 0.00 to 0.94, mean of 0.017). All but one observation borehole (site 51) showed significant (95%) alpha values for P1 wavelet power. Lower than average P1 wavelet powers were most prevalent in the Sandstone lithology (6 out of 12 sandstone sites), Greensands (1 out of 2 sites) and to some extent, the Chalk (6 out of 35 sites). It should be noted, however, that the relatively small sample sizes of Greensand and Oolite aquifers makes interpretation of systematic differences at these lithographies difficult. P1 wavelet power was generally lower across all the corresponding rainfall time series, which is expected given rainfall's established bias towards high-frequency variability (Meinke et al. 2005). Of those boreholes with lower P1 power in groundwater, most (e.g. 35, 59) show greater P1 powers in rainfall (and PET) indicating hydrogeological processes as the mechanism for weaker P1 periodicity. However, a small number (e.g. 38, 40 and 42) had similarly low P1 periodicity in the corresponding

rainfall, indicating meteorological drivers for poor annual strength at these observation boreholes (considering that PET showed little variance in P1 strength across the observation boreholes). PET spectra and alpha values showed a universally high P1 wavelet power.

The second greatest wavelet power across the groundwater boreholes was between 6 and 9 years, roughly centred on the 7 year periodicity (P7)). Maximum normalised groundwater wavelet powers ranging from 0.01 to 1 (average of 0.52) between boreholes were detected, and a corresponding band of lower than average alpha values (ranging from 0.01 to 0.99, mean of 0.34), indicating that this periodicity is likely to be driven by an external variance. Average P7 wavelet power values were greatest for Sandstone (0.68) and Greensands (1.00), and lower for Limestone (0.39) and Oolite (0.17). Chalk showed intermediate strength with the greatest range (0.01 to 1.00, mean of 0.50). Ten groundwater sites showed significant (95%) P7 wavelet powers (sites 1, 12, 14, 19, 26, 27, 49, 53, 55 and 59). While the P7 wavelet power in the corresponding rainfall data was considerably lower than those detected in groundwater level (ranging from 0.014 to 0.35, mean of 0.16), the alpha values are comparable with the P7 signal strength in groundwater. This indicates that P7 signals in rainfall are weak, but likely driven externally. Generally lower alpha values for P7 in rainfall, compared to groundwater, are also likely a result of rainfall's lower autocorrelation. Negligible wavelet powers and no significance was shown at the P7 band for corresponding PET data.

The final and second mode of common multi-annual wavelet power was the band between 16 years and 32 years (P16-32). P16-32 had an average wavelet power of 0.28 across all boreholes; ranging between 0.01 and 1. Similar to P7, the greatest wavelet power of P16-32 was found in the Sandstone (average of 0.58) and the Greensand (average of 0.64) aquifer types. Whereas Chalk, Limestone and Oolite showed relatively weaker signals (averages of 0.18, 0.32 and 0.03 respectively). Only one site in the groundwater (site 50) and five rainfall time series (sites 3, 11, 30, 34, 40) showed 95% significance over red noise in this periodicity band.

293

294 **3.2. Reconstructed anomaly time series**

295 The three main common period domains identified by the wavelet transform (P1, ~7 and 16-
296 32 years) were reconstructed into anomaly time series using the reversed wavelet transform
297 and are presented in figure 4 for groundwater levels and figure 5 for rainfall and PET. This
298 was undertaken to allow investigation and comparison of periodic behaviour over time and to
299 assess how these reconstructed periodic signals, within multiple sites across multiple aquifers,
300 align with periods of historical groundwater drought. The behaviour of the multiple
301 reconstructed groundwater level, precipitation and PET anomaly time series (in all three
302 periodicity domains) were shown to be well-aligned in time, with positive (maxima) and
303 negative (minima) phases occurring within comparable time. The only exception to this pattern
304 was seen between 1970 and 1980 in the P7 reconstructions, where phases in the P7
305 reconstructions become misaligned. This was predominantly apparent in groundwater and to
306 a lesser extent in rainfall. Positive and negative phases of the P7 reconstructions in PET were
307 well-aligned for the entire time series.

308 Notable episodes of groundwater droughts in the UK were overlaid onto the reconstructed
309 periods in figure 5 between 1955 and 2016. With the exception of the 1975-6 event, every
310 episode of drought in this time period coincides with a negative phase of the reconstructed P7
311 groundwater anomalies. The 1975-6 drought (often used as a benchmark drought in the UK
312 due to its wide-reaching impacts (Marsh et al. 2007)) occurred at a time of notable
313 minima/maxima misalignment of the P7 period across all groundwater sites, and a period of
314 negative anomaly in the P16-32 reconstructions. Most recorded major droughts in the UK
315 appeared to occur irrespective of the state of the P16-32 anomaly, with droughts occurring in
316 minima and maxima of this reconstruction.

317 **3.3. Percentage standard deviation**

The percentage of the standard deviation in the original groundwater level signal represented by each reconstructed periodicity band is shown in figure 6 for all the observation boreholes. The percentages are representative of the absolute strength of the periodicity compared to the recorded data variance (standard deviation).

P1 represents the greatest average contribution to groundwater variability across all the aquifer groups (Chalk: 41%, Limestone: 40%, Oolite: 52%, Sandstone: 26%, Greensand: 28%). While most sites show that P1 accounts for the greatest proportion of the standard deviation, P7 is the dominant periodicity at 11 of the 59 sites (5 within Sandstone, 5 within Chalk and 1 within Greensand), and P16-32 is the strongest cycle in 3 of the 59 sites (3 within Sandstone and 1 within Limestone). P1 strength in the Chalk appears to be greatest in the South of England, with weaker strengths in the South East and East. Aside from the Chalk, there are no clear spatial patterns in P1 strength. P7 accounts for an average of 21.7% of signal strength across all aquifer groups, ranging from 3.8% to 40% across the observation boreholes. Spatial variance in P7 signal strength is less when compared to P1, although there is a noted area of significance in Chalk of South East England (e.g. the Chiltern Hills and Cambridgeshire), and a smaller cluster of P7 significance in the Sandstone of the central England, where the greatest P7 strengths are found. P16-32 strengths are spatially focused in Eastern England for the Chalk, and the central and north-western England for the Sandstone. No clear patterns for the remaining aquifer groups is apparent for the 16-32 year periodicity band.

4. Discussion

4.1. Characterisation of signal presence and strength in groundwater level

Many studies have focused on the role of seasonality in defining groundwater variability, and the onset and severity of groundwater drought (Jasechko et al. 2014; Hund et al. 2018; Mackay et al. 2015; Ferguson & Maxwell 2010). While we show that the annual cycle is an important component of groundwater response, it is often not representative of overall behaviour, accounting for (on average) less than half of total groundwater level variability. Conversely, we show that multi-annual periodicities form an unprecedented proportion of total groundwater variability; with 41% of sites (24 out of 59) exhibiting multi-annual periodicity strength that is comparable to (within 10%), or greater than, seasonality. It is expected that the strength of multi-annual cycles in groundwater level will vary according to signal strength in recharge drivers (e.g. rainfall and evapotranspiration) and hydrogeological processes that lag or attenuate long-term changes in these recharge signals (Van Loon 2013; Van Loon 2015; Townley 1995; Dickinson et al. 2014). These two processes may explain the local differences in signal strength between sites in aquifer types and geographically across the UK, as displayed in our results. For instance, pronounced multi-annual variability (significant 7 year cycles and stronger 16-32 year cycles) in the Chalk sites is generally associated with catchments of thicker unsaturated zones, larger interfluves or areas of weaker corresponding seasonality in rainfall (for example, the Chiltern Hills in South East England). These catchment properties have been shown to dampen higher frequency variability between rainfall and groundwater response due to storage buffers, thereby producing a sensitivity to multi-annual variability (Peters et al. 2006; Van Loon 2013). Multi-annual cycles are also generally strong for the granular porosity aquifers (Sandstone and Greensand); which is to be expected given the influence of lower hydraulic diffusivity (typical of granular porosity flow) on the suppression of high-frequency variability (Townley 1995). This also agrees with Bloomfield & Marchant (2013) who document sensitivity to long-term accumulation in rainfall in UK Sandstone aquifers. Conversely, the Limestone and Oolite aquifer types exhibit weaker multi-annual

periodicities in groundwater level, with strong seasonality. Townley (1995) and Price et al. (2005) document that, due to their faster-responding fracture porosity with low storativity, limestone lithographies have a lower damping capacity of finer-scale variability in recharge, meaning they are able to respond in-time to the strong seasonality in PET and rainfall. Our results typically show lower percentage contributions of multi-annual periodicities to total groundwater level variability than some previous international studies (Kuss & Gurdak 2014; Neves et al. 2019; 389; Velasco et al. 2015). This can be explained by potentially weaker periodicities in driving climatic circulations over Europe compared to North America (as indicated by Kuss & Gurdak (2014)), or UK-specific hydrogeological properties such as smaller aquifer size compared to North America or continental Europe, which may affect teleconnection strength (Rust et al, 2018). However, we also expect lower percentage contributions of multi-annual periodicities due to our use of unmodified groundwater level datasets prior to spectral decomposition (wavelet transform). Using unmodified level data has enabled us to represent the absolute contribution of multi-annual variability to groundwater level behaviour at each site.

4.2. Evidence for teleconnection control on multi-annual groundwater variability

Here, we discuss the evidence that the multi-annual variability present in UK groundwater level records (as previously discussed) is the result of teleconnection influences with climatic oscillations. The conceptualisation of groundwater teleconnections of Rust et al (2018) suggests that a teleconnection between the oscillatory climate systems and groundwater level would be associated with;

a) an apparent and coherent multi-annual periodicity band within groundwater sites across a wide geographical area, that aligns with known multi-annual variability in indices of climatic oscillations (for instance, the 7-year periodicity of the NAO (Hurrell et al. 2003),

b) increased likelihood that this periodicity band is the result of an external influence, and not the result of internal red-noise variability of the groundwater level time series (as indicated by Allen et al. (1996) and Meinke et al. (2005))
c) comparable signals in rainfall as established drivers for multi-annual groundwater variability, and
d) broad alignment of minima and maxima of time-reconstructed multi-annual periodicities. Some fine-scale misalignment in groundwater periodicities is expected as a result of unsaturated and saturated zone lags between rainfall and groundwater response (Van Loon 2013; Peters et al. 2006; Dickinson et al. 2014; Cuthbert et al. 2019).

The majority of groundwater level hydrographs and corresponding rainfall profiles showed a coherent band of increased periodicity strength and periodicity significance principally around the 7-year frequency range and, to a lesser extent, the 16-32 year range. The 7 year periodicity closely compares to the principle 7-year periodicity documented in the strength of the NAO's atmospheric dipole, which has been associated with multi-annual periodicities in rainfall (Meinke et al. 2005) and groundwater globally (Tremblay et al. 2011; Kuss & Gurdak 2014; Holman et al. 2011; Neves et al. 2019). Additionally, the time-reconstructions show clear temporal alignment of minima (with the exception of the 1975-6 period, which will be discussed later), indicating the wide-spread coherent influence of a climatic teleconnection. As such, we corroborate with existing research that documents the control of the NAO on UK rainfall (Alexander et al. 2005; Trigo et al. 2004), and show new evidence of the wide-spread propagation of multi-annual variability in rainfall through to spatio-temporal multi-annual groundwater variability, conceptualised by Rust et al (2018).

While the NAO is known to be the dominant mode of winter climate variability in Europe (López-Moreno et al. 2011; Alexander et al. 2005; Hurrell & Deser 2010), the second strongest is provided by the East Atlantic (EA) pattern (Wallace & Gutzler 1981). The EA is similar in frequency structure to the NAO but shifted southward, however it has been shown to exhibit

its own internal variability (Hauser et al. 2015; Tošić et al. 2016; (Moore et al., 2013). Importantly, the EA has been shown to exhibit a 16-32 year periodicity (Holman et al, 2011), and therefore aligns with the second strongest mode of multi-annual variability in groundwater and rainfall documented in this study. As such, the increased strength, significance and minima-alignment of the 16-32 year periodicity range detected in groundwater levels in this paper may be explained through a teleconnection between the EA pattern and European winter climate variability.. While the EA has received little focus in climate variability research compared to the NAO, our findings here support Krichak & Alpert (2005) who document a multi-decadal control on UK and European precipitation through shifting phases of the EA, and Holman et al (2011) who detected weak relationships between the EA and groundwater levels in the UK. Comas-Brua and McDermotta (2014) suggest that much of the multi-decadal climate variability (temperature and precipitation) in the North Atlantic region can be explained by a modulation of the NAO by the EA, which may contribute to the spatial and temporal variability seen in both the ~7 year and 16-32 year reconstructions across the borehole sites. In summary, the modes of multi-annual variability detected in the majority of UK groundwater level hydrographs and rainfall time series appear to be best explained via a teleconnection with the NAO and EA's principle periodicities.

4.3. Teleconnections as indicators for groundwater extremes

The final objective of this paper was to assess the extent to which the timing of multi-annual periodic groundwater level oscillations align with the timing of recorded groundwater droughts. To achieve this, documented periods of groundwater drought have been compared to reconstructed periodicities within groundwater level. We show principally, that every documented groundwater drought between 1955 and 2014 occurs during a negative phase of the ~7 year cycle detected in the majority of UK groundwater boreholes, with the exception of the 1975-6 drought.

Groundwater droughts are typically the result of multi-annual accumulation of rainfall deficits, with the specific timing and duration of drought (for a particular site) also driven by sub-annual

446 rainfall and evapotranspiration (Van Loon et al. 2014; Peters 2003). Marsh et al. (2007) identify
447 a multi-annual decline in rainfall for the majority of droughts in the UK over the past 60 years,
448 with rainfall deficits reaching a critical accumulation period of 2-3 years in the lead-up to
449 drought commencement (Folland et al. 2015). It is therefore to be expected that the majority
450 of droughts are captured within the negative phases of the ~7 year cycle in the groundwater
451 level anomalies, as this cycle (along with the 16-32 year cycle) represents groundwater's multi-
452 annual response to the land-atmosphere water flux. The 1975-6 drought does not fit this
453 pattern as we show a clear disruption to the ~7 year cycle during this period. This is of
454 particular interest as this event is generally acknowledged to be anomalous for the UK. The
455 severity of this event has been solely attributed to a short-term meteorological state (i.e. high-
456 pressure atmospheric blocking) in existing literature, with very little long-term decline in
457 groundwater levels (Rodda & Marsh, 2011; Bloomfield & Marchant 2013). It is therefore to be
458 expected that the 1975-6 drought did not occur during a coherent negative phase of the ~7
459 year cycle detected in groundwater levels, and that we see a more pronounced suppression
460 of seasonality during this time. Furthermore, we note that most droughts do not perfectly align
461 with the minima of this ~7 year cycle. As previously stated, the commencement of a drought
462 is dependent a combination of on multi-annual land-atmosphere water fluxes and particular
463 sub-annual hydrological conditions (Van Loon et al. 2014). Therefore, this ~7 year fluctuation
464 could be considered a cycle of increased drought risk, where groundwater resources may be
465 more sensitive to sub-annual hydrological conditions. The 16-32 year periodicity, while also a
466 representation of groundwater's multi-annual response to moisture balance, represents a
467 smaller proportion of total groundwater behaviour and as such appears less representative of
468 drought timings. Despite this, it is likely that this signal still has a role in modulating the severity
469 of the ~7 year component.

470

471 The NAO and EA's control on long-term rainfall deficits in the UK and Europe has previously
472 been identified by many studies (López-Moreno et al. 2011; Fowler & Kilsby 2002; Hurrell

1995). Here, we provide evidence to suggest that the NAO teleconnection with long-term rainfall volumes, in particular, propagates to detectable modes of groundwater level behaviour, creating episodes of increased drought risk in-line with the NAO's principle periodicity of approximately 7 years. While the effects of (non-) stationarity between the NAO, EA and UK hydrogeology have not been assessed in this study, these detected cycles may yield improved foresight into future episodes of increased drought risk in the UK. This is especially important given the proportion of groundwater level variability these cycles represent. We also note that teleconnections are not persistent and can be disrupted as exemplified by the 1975-6 drought. Our findings here agree with Parry et al (2011) who found no relationship with this drought and the NAO phase or strength. Peings & Magnusdottir (2014) suggest that atmospheric blocking prohibits the expected effects of the NAO on UK and European rainfall, which may explain both the 1975-6 drought and the disruption to the 7-year periodicity in UK groundwater (Rodda & Marsh 2011). This therefore further highlights the importance of atmospheric blocking in regulating groundwater variability in the UK (Shabbar et al. 2001).

5. Conclusions

This paper assesses the role of multi-annual variability and ocean-atmosphere systems in influencing groundwater drought. We quantify the absolute contribution of multi-annual cycles to groundwater variability, and provide new evidence for the influence of the NAO's control of European rainfall on UK groundwater drought over the past 60 years.

The wavelet transformation was used to identify and evaluate bands of periodic external influence on UK groundwater level hydrographs. We document the strength of multi-annual behaviour that align with the NAO's principal periodicity (approximately 7 years) and the EA's principal periodicity (16-32 years). We find that seasonality accounts for an average of 39% of groundwater level variance across boreholes; with 7-year cycle accounting for an average of 21%, and 16-32 years accounting for 15%. Furthermore, we show the majority of UK droughts

align with a negative phases of the 7-year cycle indicating periods of increase drought risk as part of this periodicity. In the UK, the economic regulator has implemented several measures to promote the trading of water between water supply companies to enable a more robust water supply system (OfWAT 2019; Deloitte LLP 2015). Here, we show that recursive patterns in groundwater contribute to a considerable proportion of the total groundwater level variability and therefore may provide new insights to allow undertakers of water supply to trade water further into the future, depending on teleconnection sensitivities. Such forecasted planning could help to reduce the ecological and human impacts of groundwater drought by allowing more time to plan and organised the required water transfers from areas less susceptible to teleconnection-driven drought. It is clear from our results that long-range groundwater drought forecasts via climate teleconnections present transformational opportunities to drought prediction and its management across the North Atlantic region.

Acknowledgements

This work was supported by the Natural Environment Research Council [grant numbers NE/M009009/1 and NE/L010070/1], and the British Geological Survey (Natural Environment Research Council). We acknowledge the British Geological Survey for provision of the groundwater level data, and the Centre for Ecology and Hydrology for provision of the CHESS rainfall data (https://doi.org/10.5285/33604ea0-c238-4488-813d-0ad9ab7c51ca) and CHESS PET data (https://doi.org/10.5285/8baf805d-39ce-4dac-b224-c926ada353b7). John Bloomfield publishes with the permission of the Executive Director, British Geological Survey (NERC). Mark Cuthbert acknowledges support for an Independent Research Fellowship from the UK Natural Environment Research Council (NE/P017819/1). We thank Angi Rosch and Harald Schmidbauer for making their wavelet package “WaveletComp” freely available.

The groundwater level data used in the study are from the WellMaster Database in the National Groundwater Level Archive of the British Geological Survey. The data are available

under license from the British Geological Survey at https://www.bgs.ac.uk/products/hydrogeology/WellMaster.html (last access: 26/03/2019).

References

Alexander, L. V., Tett, S.F.B. & Jonsson, T.: Recent observed changes in severe storms over the United Kingdom and Iceland. Geophysical Research Letters, 32, 1–4, https://doi.org/10.1029/2005GL022371, 2005.

Allen, M.R., Smith, L.A.: Monte Carlo SSA: Detecting irregular oscillations in the Presence of Colored Noise. Journal of Climate, 9, 3373–3404, https://doi.org/10.1175/1520-0442(1996)009<3373:MCSDIO>2.0.CO;2, 1996.

Bloomfield, J.P. & Marchant, B.P.: Analysis of groundwater drought building on the standardised precipitation index approach. Hydrology and Earth System Sciences, 17, 4769–4787, https://doi.org/10.5194/hess-17-4769-2013, 2013

Cuthbert, M.O., Gleeson, T., Moosdorf, N., Befus, K.M., Schneider, A., Hartmann, J. & Lehner, B.: Global patterns and dynamics of climate–groundwater interactions. Nature Climate Change, 9, 137–141, https://doi.org/10.1038/s41558-018-0386-4, 2019

Deloitte LLP: Water trading - scope, benefits and options - Final Report. Deloitte LLP, 117 pp, 2015.

Dickinson, J.E., Ferré, T.P.A., Bakker, M. & Crompton, B.: A Screening Tool for Delineating Subregions of Steady Recharge within Groundwater Models. Vadose Zone Journal, 13, 1-15, https://doi.org/10.2136/vzj2013.10.0184, 2014.

Faust, J.C., Fabian, K., Milzer, G., Giraudeau, J. & Knies, J.: Norwegian fjord sediments reveal NAO related winter temperature and precipitation changes of the past 2800

548 years. Earth and Planetary Science Letters, 435, 84–93,
549 https://doi.org/10.1016/j.epsl.2015.12.003, 2016.

550 Ferguson, I.M. & Maxwell, R.M.: Role of groundwater in watershed response and land
551 surface feedbacks under climate change. Water Resources Research, 46(8), 1–15,
552 https://doi.org/10.1029/2009WR008616, 2010.

553 Folland, C.K., Hannaford, J., Bloomfield, J.P., Kendon, M., Svensson, C., Marchant,
554 B.P., Prior, J. & Wallace, E.: Multi-annual droughts in the English Lowlands: a review of their
555 characteristics and climate drivers in the winter half-year. Hydrology and Earth System
556 Sciences, 19, 2353–2375, https://doi.org/10.5194/hess-19-2353-2015, 2015.

557 Forootan, E., Khaki, M., Schumacher, M., Wulfmeyer, V., Mehrnegar, N., van Dijk,
558 A.I.J.M., Brocca, L., Farzaneh, S., Akinluyi, F., Ramillien, G., Shum, C.K., Awange, J. &
559 Mostafaie, A.: Understanding the global hydrological droughts of 2003–2016 and their
560 relationships with teleconnections. Science of the Total Environment, 650, 2587-260,
561 https://doi.org/10.1016/j.scitotenv.2018.09.231, 2018.

562 Fritier, N., Massei, N., Laignel, B., Durand, A., Dieppois, B. & Deloffre, J.: Links
563 between NAO fluctuations and inter-annual variability of winter-months precipitation in the
564 Seine River watershed (north-western France). Comptes Rendus - Geoscience, 344, 396–
565 405, https://doi.org/10.1016/j.crte.2012.07.004, 2012.

566 UK Hydrological Status Update - early July 2018: https://www.ceh.ac.uk/news-and-
567 media/blogs/uk-hydrological-status-update-early-july-2018, 2018.

568 Hauser, T., Demirov, E., Zhu, J. & Yashayaev, I.: North Atlantic atmospheric and
569 ocean inter-annual variability over the past fifty years - Dominant patterns and decadal shifts.
570 Progress in Oceanography, 132, 197–219, https://doi.org/10.1016/j.pocean.2014.10.008,
571 2015.

572 Holman, I., Rivas-Casado, M., Bloomfield, J.P. & Gurdak, J.J.: Identifying non-
573 stationary groundwater level response to North Atlantic ocean-atmosphere teleconnection
574 patterns using wavelet coherence. Hydrogeology Journal, 19, 1269–1278,
575 https://doi.org/10.1007/s10040-011-0755-9, 2011.

576 Holman, I.P., Rivas-Casado, M., Howden, N.J.K., Bloomfield, J.P. & Williams, A.T.:
577 Linking North Atlantic ocean-atmosphere teleconnection patterns and hydrogeological
578 responses in temperate groundwater systems. Hydrological Processes, 23, 3123–3126,
579 https://doi.org/10.1002/hyp.7466, 2009.

580 Hund, S. V., Allen, D.M., Morillas, L. & Johnson, M.S.: Groundwater recharge indicator
581 as tool for decision makers to increase socio-hydrological resilience to seasonal drought.
582 Journal of Hydrology, 563, 1119–1134, https://doi.org/10.1016/j.jhydrol.2018.05.069, 2018.

583 Hurrell, J.W. & Deser, C.: North Atlantic climate variability: The role of the North Atlantic
584 Oscillation. Journal of Marine Systems, 79, 231–244,
585 https://doi.org/10.1016/j.jmarsys.2008.11.026, 2010.

586 Hurrell, J.W., Kushnir, Y., Ottersen, G. & Visbeck, M.: An Overview of the North Atlantic
587 Oscillation. In The North Atlantic Oscillation: Climatic Significance and Environmental Impact.
588 American Geophysical Union, 1–35, 2003.

589 Jasechko, S., Birks, S.J., Gleeson, T., Wada, Y., Fawcett, P.J., Sharp, Z.D.,
590 McDonnell, J.J. & Welker, J.M.: The pronounced seasonality of global groundwater recharge.
591 Water Resources Research, 50, 8845–8867, https://doi.org/10.1002/2014WR015809, 2014.

592 Jelena Luković, Branislav Bajat, Dragan Blagojević, M.K.: Spatial pattern of North
593 Atlantic Oscillation impact on rainfall in Serbia. Spatial Statistics. 14, 39-52,
594 https://doi.org/10.1016/j.spasta.2015.04.007, 2014.

595 Kingston, D.G., McGregor, G.R., Hannah, D.M. & Lawler, D.M.: River flow
596 teleconnections across the northern North Atlantic region. Geophysical Research Letters, 33,
597 1–5, https://doi.org/10.1029/2006GL026574, 2006.

598 Knippertz, P., Ulbrich, U., Marques, F. & Corte-Real, J.: Decadal changes in the link
599 between El Niño and springtime North Atlantic oscillation and European–North African rainfall.
600 International Journal of Climatology, 23, 1293–1311, https://doi.org/10.1002/joc.944, 2003.

601 Krichak, S.O. & Alpert, P.: Decadal Trends in the East Atlantic-West Russia Pattern
602 and Mediterranean Precipitation. International Journal of Climatology. International Journal of
603 Climatology, 25, 183–192, https://doi.org/10.1002/joc.1124, 2005.

604 Kuss, A.M. & Gurdak, J.J.: Groundwater level response in U.S. principal aquifers to
605 ENSO, NAO, PDO, and AMO. Journal of Hydrology, 519, 1939–1952,
606 https://doi.org/10.1016/j.jhydrol.2014.09.069, 2014.

607 Lee, H.F. & Zhang, D.D.: Relationship between NAO and drought disasters in
608 northwestern China in the last millennium. Journal of Arid Environments, 75, 1114–1120,
609 https://doi.org/10.1016/j.jaridenv.2011.06.008, 2011.

610 López-Moreno, J.I., Vicente-Serrano, S.M., Morán-Tejeda, E., Lorenzo-Lacruz, J.,
611 Kenawy, A. & Beniston, M.: Effects of the North Atlantic Oscillation (NAO) on combined
612 temperature and precipitation winter modes in the Mediterranean mountains: Observed
613 relationships and projections for the 21st century. Global and Planetary Change, 77, 62–76,
614 https://doi.org/10.1016/j.gloplacha.2011.03.003, 2011.

615 Mackay, J.D., Jackson, C.R., Brookshaw, A., Scaife, A.A., Cook, J. & Ward, R.S.:
616 Seasonal forecasting of groundwater levels in principal aquifers of the United Kingdom.
617 Journal of Hydrology, 530, 815–828, https://doi.org/10.1016/j.jhydrol.2015.10.01, 2015.

618 Marsh, T., Cole, G. & Wilby, R.: Major droughts in England, 1800 - 2006. Weather, 62,
619 https://doi.org/10.1002/wea.67, 2007.

Marsh, T. & Hannaford, J.: UK Hydrometric Register. Hydrological data UK series. Centre for Ecology and Hydrology, 214 pp, 2008.

Meinke, H., deVoil, P., Hammer, G.L., Power, S., Allan, R., Stone, R.C., Folland, C. & Potgieter, A.: Rainfall variability of decadal and longer time scales: Signal or noise? Journal of Climate, 18, 89–90, https://doi.org/10.1175/JCLI-3263.1, 2005.

Neves, M.C., Jerez, S. & Trigo, R.M.: The response of piezometric levels in Portugal to NAO, EA, and SCAND climate patterns. Journal of Hydrology, 568, 1105–1117, https://doi.org/10.1016/j.jhydrol.2018.11.054, 2019.

Water Trading: https://www.ofwat.gov.uk/regulated-companies/markets/water-bidding-market/water-trading, 2019.

Pasquini, A.I., Lecomte, K.L., Piovano, E.L. & Depetris, P.J.: Recent rainfall and runoff variability in central Argentina. Quaternary International, 158, 127–139, https://doi.org/10.1016/j.quaint.2006.05.021, 2006.

Peings, Y. & Magnusdottir, G.: Forcing of the wintertime atmospheric circulation by the multidecadal fluctuations of the North Atlantic Ocean. Environmental Research Letters, 9, 34018, http://dx.doi.org/10.1088/1748-9326/9/3/034018, 2014.

Peters, E., Bier, G., van Lanen, H.A.J. & Torfs, P.J.J.F.: Propagation and spatial distribution of drought in a groundwater catchment. Journal of Hydrology, 321, 257–275, https://doi.org/10.1016/j.jhydrol.2005.08.004, 2006.

Price, M., Downing, R.A. & Edmunds, W.M.: The chalk as an aquifer. In The hydeogeology of the Chalk of North-West Europe, Clarendon Press, Oxford, 2005.

Rashid, M.M., Beecham, S. & Chowdhury, R.K.: Assessment of trends in point rainfall using Continuous Wavelet Transforms. Advances in Water Resources, 82, 1-15, https://doi.org/10.1016/j.advwatres.2015.04.006, 2015.

644 Rey, D., Pérez-Blanco, C.D., Escriva-Bou, A., Girard, C. & Veldkamp, T.I.E.: Role of
645 economic instruments in water allocation reform: lessons from Europe. International Journal
646 of Water Resources Development, 35, 1–34,
647 https://doi.org/10.1080/07900627.2017.1422702, 2018.

648 Robinson, E.L., Blyth, E., Clark, D.B., Comyn-Platt, E., Finch, J. & Rudd, A.C.: Climate
649 hydrology and ecology research support system potential evapotranspiration dataset for Great
650 Britain (1961 - 2015) [CHESS-PE], Centre for Ecology and Hydrology,
651 https://doi.org/10.5285/8baf805d-39ce-4dac-b224-c926ada353b7, 2016.

652 Robinson, E.L., Blyth, E.M., Clark, D.B., Finch, J. & Rudd, A.C.: Trends in atmospheric
653 evaporative demand in Great Britain using high-resolution meteorological data, Hydrology and
654 Earth System Sciences, (21), 1189-1224, https://doi.org/10.5194/hess-21-1189-2017, 2017

655 Rodda, J. & Marsh, T.: The 1975-76 Drought - a contemporary and retrospective
656 review. Centre for Ecology and Hydrology, 2011.

657 Rosch, A. & Schmidbauer, H.: *WaveletComp 1.1: a guided tour through the R package,*
658 *2018.*

659 Rust, W., Holman, I., Corstanje, R., Bloomfield, J. & Cuthbert, M.: A conceptual model
660 for climatic teleconnection signal control on groundwater variability in Europe. Earth-Science
661 Reviews, 177, 164–174, https://doi.org/10.1016/j.earscirev.2017.09.017, 2018.

662

663 Shabbar, A., Huang, J. & Higuchi, K.: The relationship between the wintertime North
664 Atlantic oscillation and blocking episodes in the North Atlantic. International Journal of
665 Climatology, 21, 355–369. https://doi.org10.1002/joc.612, 2001

666

667 Su, L., Miao, C., Borthwick, A.G.L. & Duan, Q.: Wavelet-based variability of Yellow
668 River discharge at 500-, 100-, and 50-year timescales. Gondwana Research, 49, 94–105,
669 https://doi.org/10.1016/j.gr.2017.05.013, 2017.

670 Szolgayova, E., Parajka, J., Blo¨schl, G. & Bucher, C.: Long term variability of the
671 Danube River flow and its relation to precipitation and air temperature. Journal of Hydrology,
672 519, 871–880, https://doi.org/10.1016/j.jhydrol.2014.07.047, 2014.

673 Tanguy, M., Dixon, H., Prosdocimi, I., Morris, D. & Keller, V.D.J.: Gridded estimates of
674 daily and monthly areal rainfall for the United Kingdom (1890 - 2015) [CEH-GEAR]. Centre for
675 Ecology and Hydrology, https://doi.org/10.5285/33604ea0-c238-4488-813d-0ad9ab7c51ca,
676 2016.

677 Todd, B., Macdonald, N., Chiverrell, R.C., Caminade, C. & Hooke, J.M.: Severity,
678 duration and frequency of drought in SE England from 1697 to 2011. Climatic Change, 121,
679 673–687, https://doi.org/10.1007/s10584-013-0970-6, 2013.

680 Tošić, I., Zorn, M., Ortar, J., Unkašević, M., Gavrilov, M.B. & Marković, S.B.: Annual
681 and seasonal variability of precipitation and temperatures in Slovenia from 1961 to 2011.
682 Atmospheric Research, 168, 220–233, https://doi.org/10.1016/j.atmosres.2015.09.014, 2016.

683 Townley, L.R.: The response of aquifers to periodic forcing. Advances in Water
684 Resources, 18, 125–146, https://doi.org/10.1016/0309-1708(95)00008-7, 1995.

685 Tremblay, L., Larocque, M., Anctil, F. & Rivard, C.: Teleconnections and interannual
686 variability in Canadian groundwater levels. Journal of Hydrology, 410, 178–188,
687 https://doi.org/10.1016/j.jhydrol.2011.09.013, 2011.

688 Trigo, R.M., Pozo-Vazquez, D., Osborn, T.J., Castro-Diez, Y., Gamiz-Fortis, S. &
689 Esteban-Parra, M.J.: North Atlantic oscillation influence on precipitation, river flow and water
690 resources in the Iberian Peninsula. International Journal of Climatology, 24, 925–944,
691 https://doi.org/10.1002/joc.1048, 2004.

692 Van Loon, A.F.: Hydrological drought explained. Wiley Interdisciplinary Reviews:
693 Water, 2, 359–392, https://doi.org/10.1002/wat2.1085, 2015.

694 Van Loon, A.F.*On the propagation of drought: How climate and catchment*
695 *characteristics influence hydrological drought development and recovery*. Ph.D thesis.
696 Wageningen University, 2013.

697 Van Loon, A.F., Tijdeman, E., Wanders, N., Van Lanen, H.A.J., Teuling, A.J. &
698 Uijlenhoet, R.: How climate seasonality modifies drought duration and deficit. Journal of
699 Geophysical Research-Atmospheres, 119, 4640–4656,
700 https://doi.org/10.1002/2013JD020383, 2014.

701 Velasco, E.M., Gurdak, J.J., Dickinson, J.E., Ferré, T.P.A. & Corona, C.R.: Interannual
702 to multidecadal climate forcings on groundwater resources of the U.S. West Coast. Journal of
703 Hydrology: Regional Studies, 159, 16, https://doi.org/10.1016/j.ejrh.2015.11.018, 2015.

704 Wallace, J.M. & Gutzler, D.S.: Teleconnections in the Geopotential Height Field during
705 the Northern Hemisphere Winter. Monthly Weather Review, 109, 784–812,
706 https://doi.org/10.1175/1520-0493(1981)109%3C0784:TITGHF%3E2.0.CO;2, 1981.

707 Wang, H., Chen, Y., Pan, Y. & Li, W.: Spatial and temporal variability of drought in the
708 arid region of China and its relationships to teleconnection indices. Journal of Hydrology, 523,
709 283–296, https://doi.org/10.1016/j.jhydrol.2015.01.055, 2015.

710 Weber, K. & Stewart, M.: A Critical Analysis of the Cumulative Rainfall Departure
711 Concept, Groundwater, 42, 935-938, https://doi.org/10.1111/j.1745-6584.2004.t01-11-.x,
712 2004.

713